

# COMBINATION OF TWO ECRIS CALCULATIONS: PLASMA ELECTRONS AND EXTRACTED IONS

S. Biri, R. Rácz, Atomki, Debrecen, Hungary  
P. Spädtke, K. Tinschert, R. Lang, J. Mäder, F. Maimone and B.R. Schlei,  
GSI, Darmstadt, Germany

## Abstract

In strongly magnetized ECRIS plasmas collisions do not influence the path of the charged particle. Electrons and ions can move more freely only along a magnetic field line compared to the transverse direction. Therefore, extraction simulation requires that the trajectories of charged particles have to be traced through the plasma chamber instead of starting at the plasma boundary. In previous simulations the particle density at the beginning of the trajectory deep inside the plasma has been unknown. Now the full 3D electron tracking within the plasma chamber has been combined with the generation of initial ion starting conditions including particle density for ion tracking. The TrapCAD code has been used to determine the electron spatial distribution in a certain energy window. The idea is that at the places where the electron reaches a specific energy, an ion trajectory can be started. The magnetic field has been modeled with OPERA, whereas for solving the electric potential and the particle tracking the computer code KOBRA3-INP has been used. First results will be shown and discussed. The number of affecting parameters on the operating conditions of the ion source may lead to a multi-dimensional optimization space for simulation.

## MOTIVATION

Several attempts have been done in the past to simulate the extraction of ions from an Electron Cyclotron Resonance (ECR) Ion Source (ECRIS). Most of these attempts gave only partial results or even failed, because they were not able to reproduce the experimental results. In early simulations the ions started from outside the plasma or just at the plasma boundary. Later models tried to include the effect of the non-cylindrical magnetic field [1]. One of the recent and best models up to now is given by the following procedure: tracing magnetic field lines through the extraction aperture, looking where these field lines are coming from, and using the coordinates of the magnetic field line as starting points for ions to be extracted [2]. This means magnetized ions are considered.

It is also also well-known that energetic plasma electrons are strongly tighten to the magnetic field lines. The question is whether we can use the coordinates of these electrons by simultaneously using the field lines? A simulation study of ECRIS plasma electrons revealed that in certain cases the positions of the electrons inside the plasma chamber may correspond to the positions of the highly charged ions [3]. The study was built on direct experimental results: on visible-light photos and on energy-filtered X-ray photos of argon plasmas.

In this paper we make an attempt to combine the two methods: a plasma electron cloud is simulated in a given ECRIS configuration and the coordinates of these electrons are used to be the starting positions of ions to be extracted. During the extraction procedure the fully 3D magnetic field structure of the ECRIS (inside and outside the plasma) is taken into account.

## THE ECRIS CONFIGURATION

For the simulations of plasma electrons and ions to be extracted the CAPRICE-type ECR ion source operating at GSI was selected. The technical details of this ECRIS are described elsewhere [4]. It has a relatively short plasma chamber in a strong magnetic trap (created by two room-temperature coils and by a NdFeB-magnet hexapole) operating on 14.5 GHz microwave frequency (even it is suitable to operate at different frequencies) [4]. The simulation of electron movement requires the knowledge of magnetic field values in a fine 3D mesh. Because ECRISs have certain symmetries, for this pre-calculation a real 3D code was not necessary. Instead, the 2D PoissonSuperfish code (version 6.15) has been used [5]. For the calculation the exact geometry of the GSI-CAPRICE with typical coils currents used for highly charged ion production were applied (see Table 1).

Table 1: Input parameters for Superfish calculations

Parameters for calculation	Value
Plasma chamber length:	187 mm
Plasma chamber diameter:	63 mm
Injection coil current:	1100 A
Extraction coil current:	1100 A
Hexapole materials (VACODYM):	745HR/655HR
Mesh size for the coils system:	0.5 mm
Mesh size for the hexapole system:	0.2 mm

Figure 1 and 2 show the result: the geometries of the axial and radial magnetic traps and the relevant magnetic field distributions. Throughout with Superfish and TrapCAD calculations in this paper the axis of the plasma chamber is marked by  $z$  and the radial distance is marked by  $r$ . The calculated magnetic curves correspond well (inside the plasma chamber) with measurements carried out by the GSI team earlier. The curves show the minimum and maximum values of the magnetic field

inside the plasma chamber. These values with different mirror ratios ( $B_{max}/B_{min}$ ) effect the production of ions.

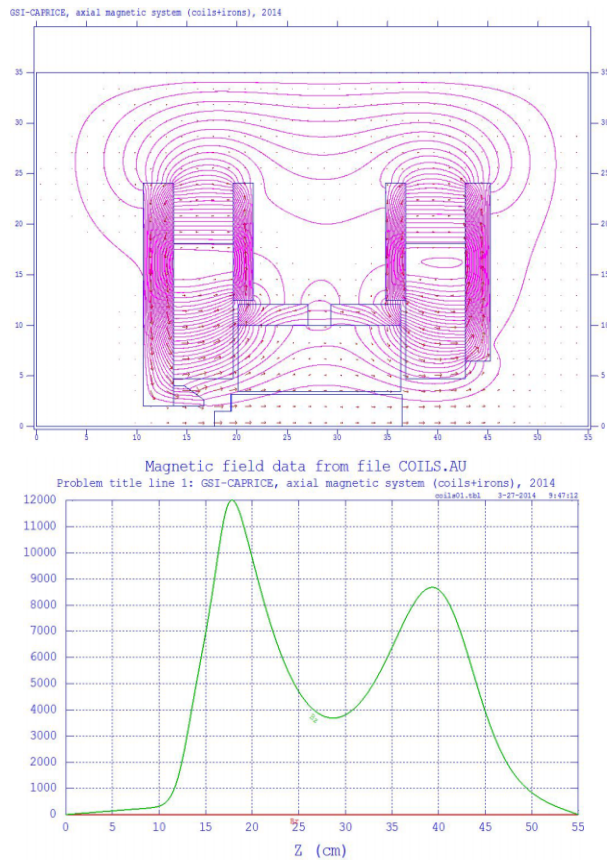


Figure 1: The axial magnetic trap (coils+irons) of GSI-CAPRICE calculated by PoissonSuperfish, injection side left. Down: axial magnetic field curve.

### THE TRAPCAD CODE

The superposition of the two components of the GSI-CAPRICE magnetic field was then made including the end-effects of the hexapole magnet in order to get a realistic fine-meshed 3D magnetic array. The special movement and energy-evolution of a high number of electrons were then simulated by the TrapCAD code which was developed and several times upgraded by the Atomki team. Details of the code are fully described in paper [3] and in its references.

TrapCAD was made to visualize the magnetic trap structure of ECR and other ion sources and to follow the energy and spatial evolution of electrons. It is a limited 3D code which means the magnetic system must have some regularities (cylindrical axial field, multipolar radial field), but the resulting motion is calculated in 3D. The magnetic field has to be calculated by other pre-processing codes (usually by the PoissonSuperfish group of codes). A 4-order Runge-Kutta method is applied for the integration of the magnetic field line equation. The Lorentz force integration is processed by a time-centered leapfrog scheme explicitly solving the motion equations. The code is based on the one electron approach with

neglecting the particle-particle interactions. The electron heating (the electron-cyclotron-resonance process) is calculated by assuming a simple RF field but realistic magnetic field configuration. The electrons are heated up by stochastic resonance process. As a result, the spatial and energy structure of both the non-lost and lost electrons can be calculated. Non-lost electrons are called those which remain in the plasma chamber by the end of the simulation time. Lost-electrons hit the walls and their energy is given to the wall.

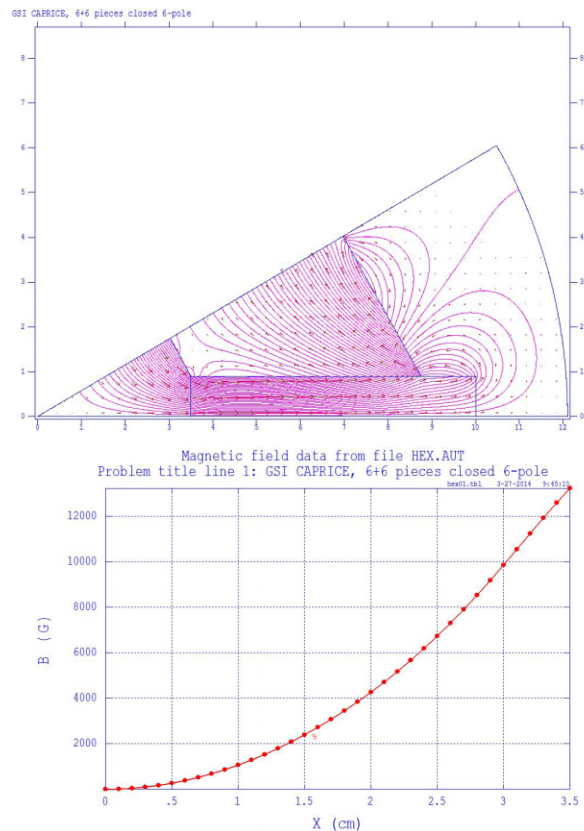


Figure 2: The radial magnetic trap of GSI-CAPRICE calculated by PoissonSuperfish (30 degrees section). Down: the radial magnetic field distribution at a pole.

In a recent work [6] of our team the simulation of the plasma electrons in the Atomki-ECR ion source [7] was carried out in a very detailed way. Graphical front and side views and plasma slices show the spatial structure of the plasma electrons [6].

### PLASMA ELECTRONS SIMULATIONS

The spatial and energy distribution of the non-lost (plasma) electrons in the 14.5 GHz GSI-CAPRICE ECRIS were calculated by TrapCAD. Four million electrons were placed with equal density into a thin layer around the closed resonance surface. The simulation time was 200 nanoseconds (a timescale such that the particle-particle interactions can be neglected). In real (CPU) time the calculation lasted for 146 hours in a PC with i7 processor. At the end of the simulation cca 40 % (1.6 million) of the electrons were still remained in the plasma

and 60 % were lost on the chamber wall. Some important parameters regarding the starting conditions of the simulation and some numerical results are in Table 2.

Table 2: I/O parameters of the TrapCAD calculations

Parameters for calculation	Value
Number of electrons:	4000000
Start position (resonant surface)	5200 +/- 200 gauss
Perp. energy components:	1 - 100 eV, random
Parallel energy components:	1 - 100 eV, random
RF frequency:	14.5 GHz
RF power:	1000 W
Simulated time:	200 ns
Number of lost particles:	2396026 (59.9 %)
Number of non-lost particles:	1603974 (40.1 %)
Average energy of lost particles:	118 eV
Av. energy of non-lost particles:	2753 eV

In the subsequent figures (figures 3-6) some direct numerical and graphical results of the TrapCAD simulation are shown.

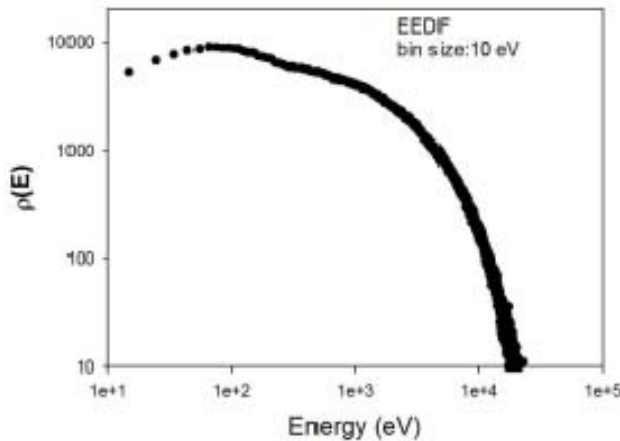


Figure 3: The electron energy distribution function (EEDF) of the non-lost electrons.

The goal and the most important result of the TrapCAD simulation was the creation of the huge non\_lost.txt ASCII file containing the starting and ending coordinates (x, y, z) and the starting and ending energy (parallel, perpendicular, total) of all non-lost electrons. This file was used as basic database for the simulation of the ions extraction.

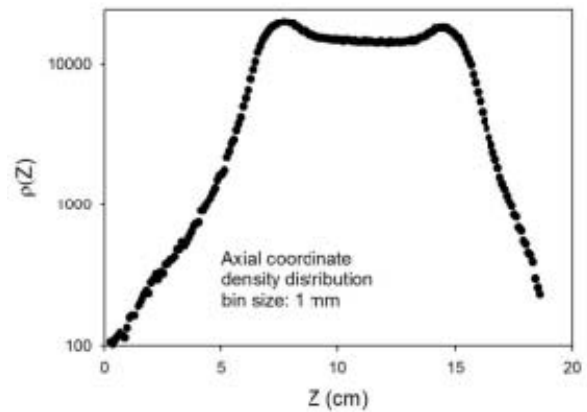


Figure 4: The axial distribution of the non-lost electrons. Left: injection side.

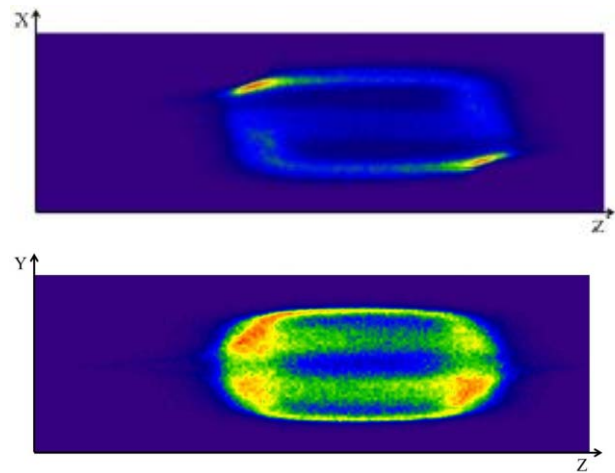


Figure 5: Radial (side-view) projection of the electron cloud from the direction of a magnetic gap (up) and from a magnetic pole (down).

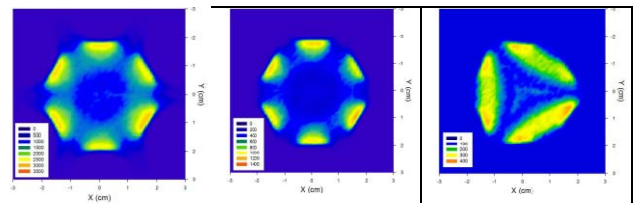


Figure 6: Axial (end-view) projection of the non-lost electrons. Left: all electrons, middle: warm electrons (3 keV < E < 10 keV), right: warm electrons close to the extraction side (Z > 13 cm).

## THE KOBRA3-INP CODE

KOBRA3-INP [8] is a fully 3-dimensional Vlasov solver. It discretizes the geometry to a Cartesian mesh. The Laplacian potential is then determined for each node. Magnetic flux density needs to be defined on each node at that time. Once the starting conditions have been defined, ray tracing can be performed. The space charge of each trajectory will be distributed to the surrounding nodes

accordingly. This space charge can then be used to calculate Poisson's equation. The space charge is assumed to be neutralized within the plasma, as well as in the extracted ion beam, if an appropriate accel-decel system has been used. As well as in a real experiment, diagnostic tools are essential to present the results. KOBRA-3 can generate (beside other diagnostics) emittance plots. Such an emittance plot is a projection of the 6-dimensional phase space into the 2D drawing plane. As an example, the vertical emittance  $\mathcal{E}_y$  is defined as:

$$\mathcal{E}_y = \iiint f(y,y') dx dz dx' dz' \quad (1)$$

where  $y$  and  $z$  are the transverse directions and  $x$  is the longitudinal direction. (Throughout with KOBRA calculations in this paper the axes of the plasma chamber is marked by  $x$ .)

Due to the coupling between planes for ECRISs it is not allowed to restrict to 2D subspaces. We do need for a correct presentation of the results at least the 4D transverse phase space (if not the 6D phase space is necessary). Such a possibility is under investigation momentarily at GSI, see the last section. Because of the coupling between planes due to the strong magnetic flux density, other projections than the typical emittances are also used which are important for accelerators:

$$\mathcal{P}_y = \iiint f(y,z') dx dz dx' dy' \quad (2)$$

$\mathcal{P}_y$  describes the coupling from the  $y$ -plane to the perpendicular one. (In Fig. 12 this coupling will be shown for different charge states.)

### TRANSFER FROM TRAPCAD TO KOBRA

It was necessary to build an interface bridge between TrapCAD and KOBRA. The final coordinates of the non-lost electrons were used to start at all of these places an ion. Each ion was started with a very low starting energy. In figure 7 the starting conditions of the ions are drawn in two views.

Altogether 1.6 million trajectories were created by this way for each charge state. From this total number 229635  $\text{Ar}^+$  ions could be extracted (14 %), 185523  $\text{Ar}^{3+}$ , (12%), 167193  $\text{Ar}^{5+}$  (10%) and 108729 p (7%). All other ions stayed in the plasma chamber. The trajectory calculations required huge disc space, the file size of trajectory coordinates (all coordinates of all trajectories along each path) in total was in the order of 26GB, for singly charged Ar, 34GB for  $\text{Ar}^{3+}$ , 28GB for  $\text{Ar}^{5+}$ , and 35GB for p. In figure 8 a typical trajectory plot is shown. The different colors indicate where the ions are coming from (black injection side, yellow and green extraction side). The figure also shows some geometry values which will be important at the emittance figures (see next chapter).

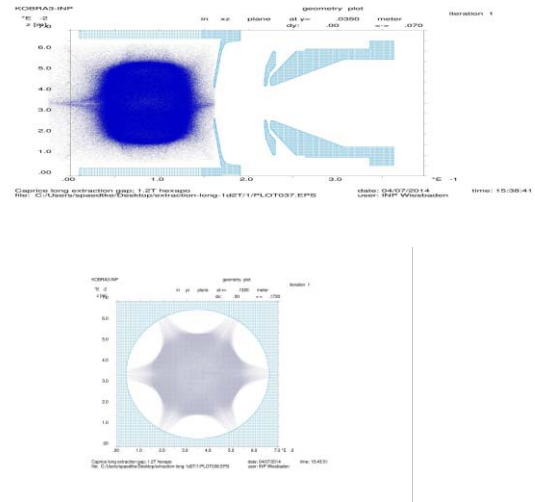


Figure 7: The starting conditions of ions. Up: side view, cut in the mid-plane, down: end view, cut in the plasma chamber. Each dot is one macro particle. Starting conditions are projected into the drawing plane.

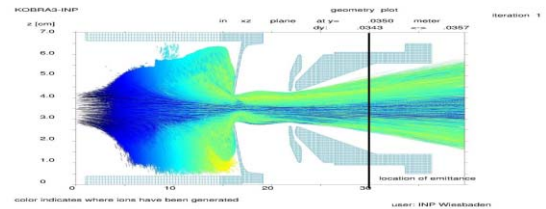


Figure 8: GSI-CAPRICE, typical trajectory plot. The ions are coming from deep inside the plasma. Black are particles coming from the injection side, blue from the middle, green and yellow from the extraction side. The emittance calculations are performed at 30cm.

### ION EXTRACTION FROM INSIDE THE PLASMA CHAMBER

The final results of the TrapCAD+KOBRA combined simulation work will appear in emittance figures. In KOBRA each phase space diagram is a projection of the 6D phase space volume into the 2D plane of drawing. As mentioned, in KOBRA  $x$  is the longitudinal direction,  $y$  and  $z$  are perpendicular to it. Because the operation mode is CW, we can forget  $x,x'$ . All emittances are given at  $x=0.3$  m,  $y=0.035$  m, and  $z=0.035$ m (see Figure 8).  $y$  and  $z$  are exactly on the middle,  $x$  is after extraction.

The following projections can be created: real space, emittance (hor and ver), mixed phase space (hor and ver), and the angle or momentum space. We are using the emittance definition as described in Eq. 1. This definition of emittances is equivalent to the hardware of the Allison scanner. However, this Cartesian interpretation is not suitable for an ECRIS, one should use a pepper pot method instead. In KOBRA we can approximate pepper pot emittances by inserting a slit (hor or ver) just at the

position  $x=0.3$  m. With that we can differentiate  $y, y'$  for different  $z$ .

In figures 9-13 different emittance drawings show the beam quality at the  $z=0.3$  m axial position.  $Ar^+$ ,  $Ar^{3+}$ ,  $Ar^{5+}$  and proton particles were calculated and are shown, the color indicates the charge state. Beam current was not included. It is clearly visible, that the typical structure of an ECRIS beam is visible already without space charge effects.

It should be mentioned, that the emittance with the above given definition for each charge state is much larger than the emittance given by the pepper pot definition. If the emittance diagnosis is limited to slices between  $n \cdot dy$  and  $(n+1) \cdot dy$  it can be seen, that it consists of a series of emittance figures with much smaller size. However, the single emittance slices do not overlap totally, and the superposition of all slices is the reason for the relatively large emittance. This is shown in Fig. 13.

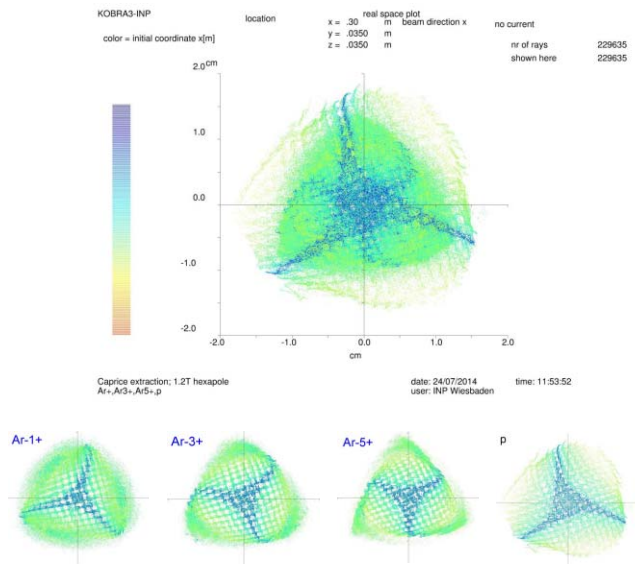


Figure 9: Real space ( $y$ - $z$ ) emittance plots. Up: all charge states. Down: individual charge states.

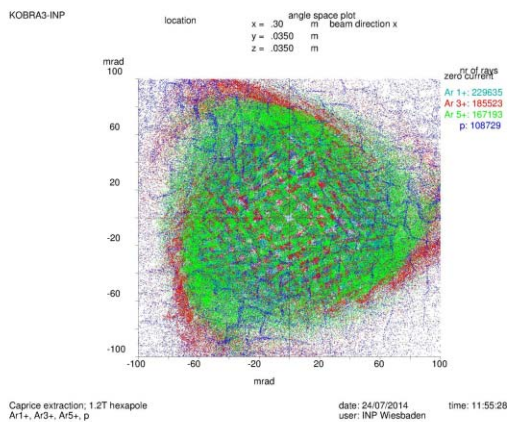


Figure 10: Momentum space ( $y'$ - $z'$ ) plot.

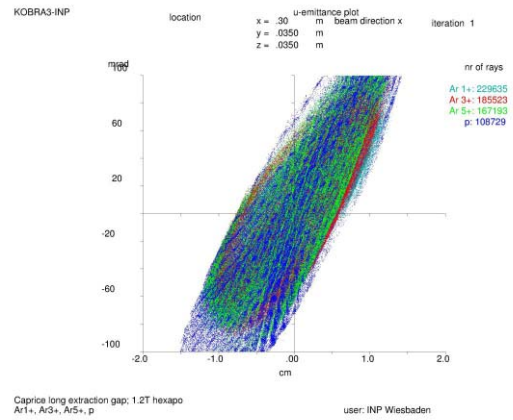


Figure 11: One of the transverse emittances,  $y, y'$ . The structure of the beam is clearly visible.

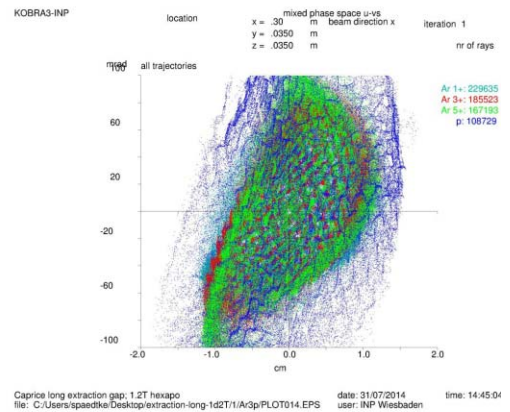


Figure 12: Mixed phase space  $y$ - $z'$ . The structure of the beam is clearly visible.

It should be mentioned, that the emittance with the above given definition for each charge state is much larger than the emittance given by the pepper pot definition. If the emittance diagnosis is limited to slices between  $n \cdot dy$  and  $(n+1) \cdot dy$  it can be seen, that it consists of a series of emittance figures with much smaller size. However, the single emittance slices do not overlap totally, and the superposition of all slices is the reason for the relatively large emittance. This is shown in Fig. 13, where different parts of the ion beam produce different emittances.

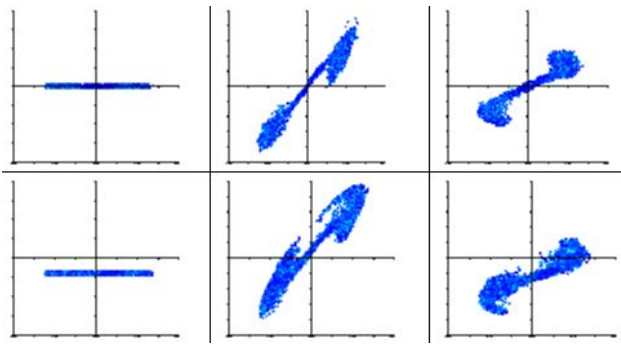


Figure 13: Left real profile ( $y$ - $z$ ), middle horizontal emittance ( $y$ - $y'$ ), right: horizontal mixed phase space ( $y$ - $z'$ ). First row: a slit selects ions only close to the vertical center, second row a slit selects ions from a negative vertical location.

### VISUALISATION IN 4 DIMENSIONS

It is possible to extract so-called iso-surfaces from three-dimensional (3D) image data (see [9] and refs. therein). The surfaces usually consist of sets of triangles, which water-tightly enclose regions of the discretized 3D data under consideration. The 3D image data are made up by so-called voxels (i.e., volume pixels). In four dimensions (4D), 4D image data are decomposed into tesseracts (or 4-cubes), and the analogous manifolds of co-dimension 1 are called hyper-surfaces. The STEVE algorithm [10] extracts hyper-hole free iso-hyper-surfaces, which consist of continuous sets of tetrahedrons that are embedded into 4D. Eventually, the hyper-surfaces themselves may be intersected with a 3D subspace, which allows for the rendering of a 3D surface with respect to an initially given iso-value and an associated intersection. The latter is in analogy to intersecting a 3D triangular iso-surface with a single plane, which then yields a curve in the two-dimensional intersecting space. Hence, one can probe the shape dependence of extracted iso-hyper-surface while visualizing (in general volume-enclosing) surfaces that correspond to various intersecting spaces. Such scans provide information about the dimensionality of the object, which is embedded into the 4D image data set and which has been enclosed by the iso-hyper-surface.

Kobra3-INP generates  $m$  arrays with rank three. Each array contains the particles having a transverse coordinate between  $m \cdot dy$  and  $(m+1) \cdot dy$ . Each element of the 3D array having a coordinate between  $n \cdot dz$  and  $(n+1) \cdot dz$ , an angle between  $o \cdot dy'$  and  $(o+1) \cdot dy'$ , and the other transverse angle between  $p \cdot dz'$  and  $(p+1) \cdot dz'$ .  $m$ ,  $n$ ,  $o$ ,  $p$  are integers. We have chosen  $m=n=o=p=50$ . Here, the iso-hyper-surface represents the “machine ellipse” of this transversal 4D phase space, which encloses all generated particles.

One can see clearly in figure 14 that the iso-hyper-surface under consideration (not directly visible here) has true four-dimensional shape features. First, the shapes in each 3D subspace are not flat, but each one of them encloses a 3D volume, and second, the shapes depend on the intersecting cube within the tesseract (i.e., the initial 4D data set).

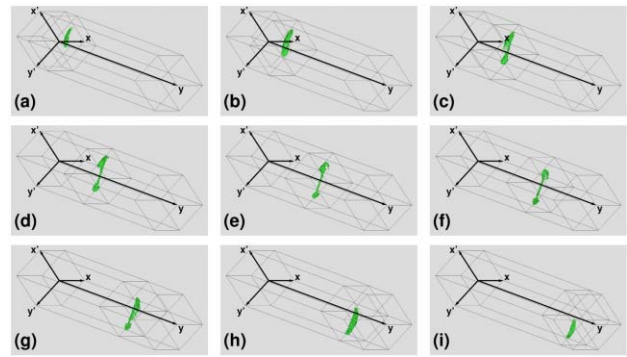


Figure 14: Intersection of the invisible iso-hyper-surface for nine different 3D subspaces (additional, interior cubes within the tesseracts). From left to right then down.

### CONCLUSION

Our work showed that to do a realistic ion extraction simulation it is necessary and possible to start the ions from inside the plasma chamber. The starting positions of the ions are developed by positions of the plasma electrons. The first ray-tracing and emittance diagrams are very promising because the known structure of an ECRIS beam could be reproduced. In the next steps the following tasks are planned to be carried out: introducing space charge, energy filtering of the electrons, concentration to specific charge states, improvement of diagnostic properties in the simulation (pepper pot diagnostic), and further comparison with experiments. The diagnostic tools will produce 4D figures, which need to be presented. However, the parameter space to be scanned by simulations is multi-dimensional, mainly because of the magnetic field distribution, gas pressure, rf coupling, charge exchange processes and further more.

### ACKNOWLEDGEMENTS

The research leading to these results has received funding from the European Union Seventh Framework Program FP7/2007-2013 under Grant Agreement n° 262010 - ENSAR. The EC is not liable for any use that can be made on the information contained herein.

### REFERENCES

- [1] Kitagawa A., Muramatsu M., Sekiguchi M., Yamada S., Jincho K., Okada T., Yamamoto M., Biri S., Uno K.: Optimization of the radial magnetic field of an 18 GHz electron cyclotron resonance ion source at the Heavy Ion Medical Accelerator in Chiba. Review of Scientific Instruments 71 (2000)2:981-983
- [2] P. Spädtke, R. Lang, J. Mäder, F. Maimone, J. Roßbach, K. Tinschert: Ion Beam Extraction from Magnetized Plasma, 20th International Workshop on ECR Ion Source. ECRIS 12. Sydney, Australia, 25-28 Sept., 2012. <http://accelconf.web.cern.ch/AccelConf/ECRIS2012/papers/weyo03.pdf>

- [3] R. Rácz, S. Biri and J. Pálincás: ECR plasma photographs as a plasma diagnostic. *Plasma Sources Sci. and Tech.* 20 (2011) 025002(7)
- [4] Maimone, F., Tinschert, K., Celona, L., Lang, R., Maeder, J., Rossbach, J., Spaedtke, P., Operation of the CAPRICE electron cyclotron resonance ion source applying frequency tuning and double frequency heating, *Review of Scientific Instruments* 83(2) (2012) 02A304
- [5] [http://laacg.lanl.gov/laacg/services/download\\_sf.phtml](http://laacg.lanl.gov/laacg/services/download_sf.phtml)
- [6] Biri S., Rácz R., Perduk Z., Vajda I., Pálincás J.: Recent developments and electron density simulations at the Atomki 14.5 GHz ECRIS. 20th International Workshop on ECR Ion Source. ECRIS 12. Sydney, Australia, 25-28 Sept., 2012. <http://accelconf.web.cern.ch/AccelConf/ECRIS2012/papers/wexo02.pdf>
- [7] S. Biri, R. Rácz and J. Pálincás: Status and special features of the Atomki ECR ion source. *Review of Scientific Instruments* 83 (2012) 02A341
- [8] KOBRA-INP, Junkernstr. 99, 65205 Wiesbaden, Germany
- [9] B. R. Schlei, Volume-Enclosing Surface Extraction, *Computers and Graphics*, 36(2), 2012, pp. 111-130, DOI: 10.1016/j.cag.2011.12.008.
- [10] B. R. Schlei, STEVE – Space-Time-Enclosing Volume Extraction, (2013) arXiv:1302.5683.